

Movement of water flux through unsaturated zones: a transient impact on *in situ* potential field

Rolland Andrade*, D. Muralidharan and R. Rangarajan

Attempts were made to understand moisture movement in soil and unsaturated zones under a transient saturation phase created through an infiltration test using conventional self-potential (SP) survey and supportive studies of resistivity profiling and tracer, over a granite terrain having coarse sandy soil cover. The SP behaviour at various time intervals of infiltration stages qualitatively indicated a preferential soil moisture movement after an initial vertical downward movement at deeper depths. As inferred from the SP survey, tracer and conventional resistivity profiling studies substantiate the flow direction by means of highest concentration of tritium content in deep soil cores and significant reduction in apparent resistivity along the direction. The results demonstrate that the SP method could be a useful tool to understand the rainfall recharge process and in surface-induced contamination studies.

Keywords: Infiltration test, soil moisture movement, water flux.

TRACING soil–water flux is essential in groundwater studies as it directly helps in understanding soil and unsaturated zone hydraulics. As water flux is highly variable in space and time, the classical hydraulic method requires numerous and repetitive measurements. Natural electrical field development due to water movement in a porous medium was demonstrated through a sandbox model laboratory controlled experiment¹. Some applications of this potential tool have been demonstrated through studies over active volcanic and tectonic regions and leakage studies in dams and lakes^{2–7}. Also, many studies established a quantitative relationship between hydraulic properties and electrical properties of a saturated regime^{8–11}. However, work on SP experiments in unsaturated zones is very limited. The combination of electric and hydraulic flows was demonstrated near an infiltration rectangular ditch through field experiments and a linear relationship between electrical potential and water table depth was established¹². Using streaming potential data numerical modelling of both hydraulic and electric processes in the vadoze zone was attempted and an inversion scheme was proposed for estimating the soil hydraulic parameters from *in situ* infiltration experiments¹³. Long-term monitoring of SP at specific depth interval in two soil types placed in lysimeters showed that variations are linked to

rainfall and evaporation processes. The slope of the water flux and SP relationship was found to vary with soil type, with the slope decreasing in electrically conductive soils¹⁴. In this study, we report the results of natural and induced electrical fields and tracer movement under a transient saturated flow condition created through an infiltration test to study the movement of moisture in soil and unsaturated zones over a sandy regolith underlined by granites.

Potential field

Self-potential develops due to the existence of a natural gradient of electric potential. This natural potential gradient is due to prevailing gradients in temperature, chemical and fluid pressure electrokinetic phenomena. SP anomalies are generally predominant in field conditions due to the electrokinetic potential gradient that exists in aquifers where groundwater movement takes place. The differential motion between the fluid and solid induces electrokinetic phenomena in a saturated medium. Aggregate of negatively charged minerals forming the porous medium, create an electric double layer in the pore fluid. The self-potential due to fluid motion in pore spaces is also called streaming potential. This is due to the motion of the diffuse layer along with fluid flow, induced by a pressure gradient. The shear planes in the fluid, i.e. the zero velocity surfaces, are located within the diffuse layer. The electric potential along this surface is called

Rolland Andrade is in the Central Water and Power Research Station, Pune 411 024, India; D. Muralidharan and R. Rangarajan are in the National Geophysical Research Institute, Hyderabad 500 007, India.

*For correspondence. (e-mail: andrade.rolland@gmail.com)

zeta potential. The contribution from the other two, namely the thermoelectric and chemical gradients, is smaller than the electrokinetic coefficient under a natural field condition^{15,16}. A quantitative relationship was seen between the circulating water and electrical potential difference when subjected to high pressure¹⁷. The linear relationship between the water flux and the electrical field was established through field experiments by measuring the electrical potential difference between the electrodes placed in the soil resting over glacial deposits at depths of 0.3 and 0.5 m with a distance of 0.2 m between them¹⁸.

Materials and methods

Field procedure

The movement and direction of soil–water flux helps understand the natural recharge process during rainy season. Moreover, high variability of water flux with time and space requires continuous monitoring of changes that occur in the soil and unsaturated zones. SP is easy to measure at regular time intervals in order to study the influence of moving soil–water flux on natural potential field. Hence point potential (PP) method of SP was adopted to trace the moving water flux simulated during an infiltration test. In order to integrate and validate the SP results, the changes in sub-surface electrical conductance at different time intervals and migration of tracer due to the infiltration process have been dovetailed with the SP survey.

A grid of 4 m × 4 m with 0.5 m grid interval was laid over a sandy soil cover followed by weathered granite. The field experiment set-up in the month of April is schematically shown in Figure 1. The PP method was adopted by keeping one of the non-polarized electrodes at infinity (at a distance of 250 m away from the grid site). The other electrode was moved along all the grid nodal points during each set of measurements. The electrodes were neutralized by placing them in a saturated ditch for a long time (~360 min) before commencing the survey. Non-polarizable electrodes (porous tubes containing saturated copper sulphate solution and a copper rod) were used for data acquisition of SP to avoid the problems occurring due to physical and chemical changes within the measuring media. Non-polarizable electrodes of 25 mm diameter were placed in pits of 30 mm diameter with a depth of 50 mm filled with sufficiently wetted *in situ* soil. A double-ring infiltrometer was placed at the centre (E-2) and the infiltration test was conducted for 180 min with a constant head of 5 cm. During the infiltration test, the potential measurements were made at regular time intervals at all the grid nodal points. Measurements were taken at all the nodal points before the start of the infiltration test. Sets of SP measurements were observed at 0, 15, 30, 45, 60, 90, 120 and 180 min of the experiment. A high

impedance voltmeter was used to measure the potential at each nodal point. The point potentials were recorded with polarity.

Infiltration test

Water entering the soil surface and percolating into deeper layers is a natural process during rainy days. However, this rate is essentially controlled by soil texture and period of water availability. The maximum rate at which the soil can absorb water is its infiltration capacity. Infiltration theory has been developed from the physics of soil–water movement based on Richard's equation¹⁹ without accounting for the effect of air phase on the water flow, and assuming the soil to be inert and isotropic. In general, infiltration begins at a higher rate and decreases to a fairly steady state level after a certain lapse of time, attaining a state of ultimate infiltration rate. The decrease in infiltration rate as a function of time was explained through mathematical analysis²⁰. The most commonly used technique in field investigations for estimation of infiltration rate of soils is the double ring infiltrometer. Two mild steel ring plates with a height of 20 cm and diameter of 20 and 40 cm were used for the experiment. The two circular plates were driven into the soil uniformly without tilt and undue disturbance of the soil surface to a depth of 5 cm by placing the smaller ring inside the bigger ring, keeping a uniform annular space between the two rings. Two point gauges were fixed; one in the centre and the other in the annular space between the two rings. In order to minimize the other two influencing factors of SP namely the chemical and thermoelectric gradients, groundwater from the region was used for conducting the infiltration test. Water was added simultaneously in the central and outer annular space for creating a height of 5 cm. The quantity of water added to maintain the height of 5 cm was noted at regular time intervals. The infiltration test was continued for 180 min till a steady state infiltration was attained. The infiltration rate was calculated using the volume of water added to maintain the height at a given time over various time intervals. The infiltration rates observed at different time intervals were tabulated and the resultant infiltration curve is shown in Figure 2.

Tritium tracer experiment

In order to trace the moisture migration with depth, tritium (HTO) tracer was used in the present experiment. Tritium, the radio isotope of hydrogen, with a half-life of 12.43 years, is used as a tracer in natural recharge studies, since it is part of the water molecule itself²¹. A quantity of 20 ml of 30 micro-curie/ml of tritium was irrigated on the surface area occupied by the inner infiltrometer ring before starting the infiltration test. During the infiltration

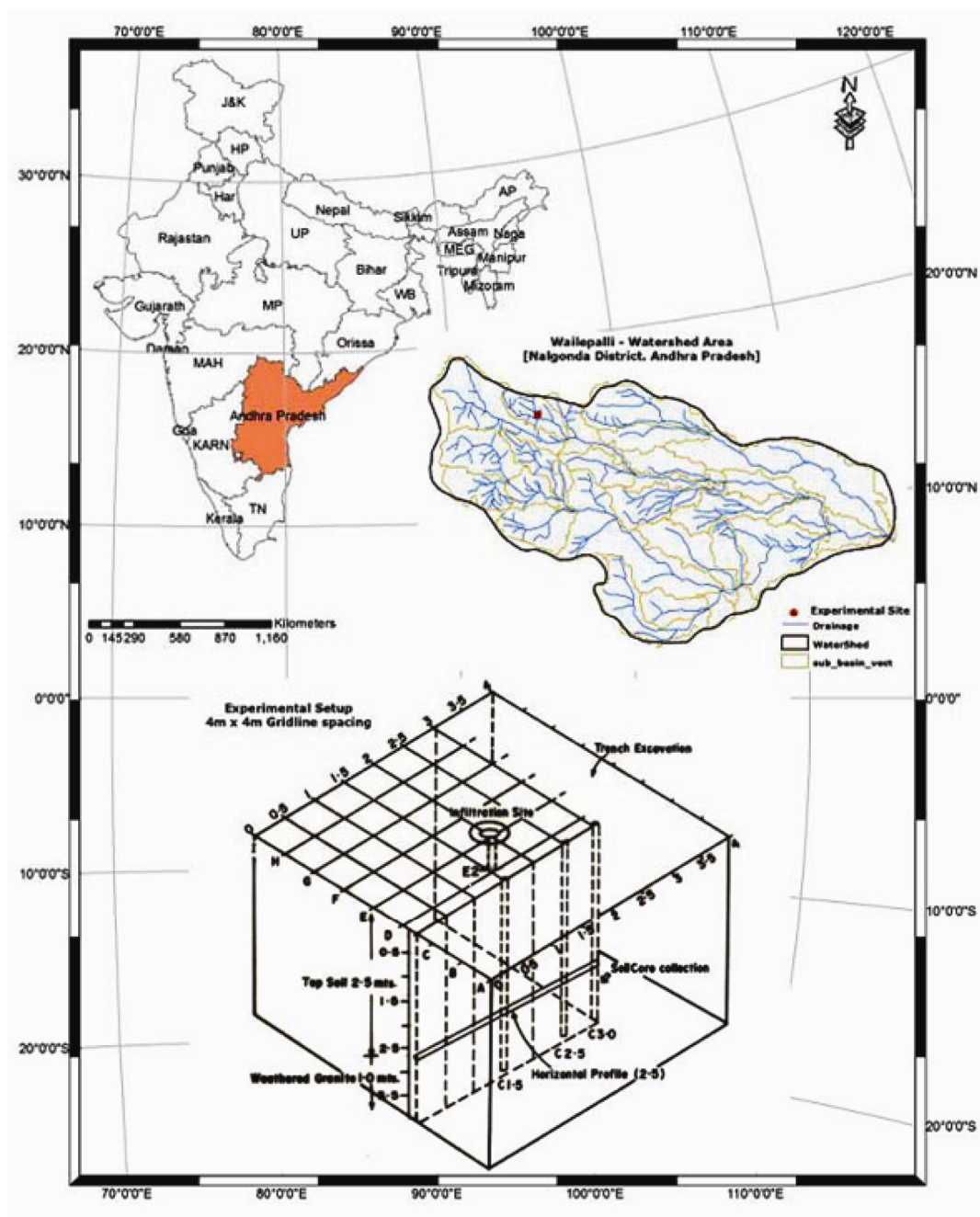


Figure 1. Location map with experimental set-up in the study area.

test the tritium tracer infiltrated along with water and percolated deeper as part of the moving flux. After the infiltration test, i.e. after 180 min, the soil core samples at various depths were collected from the central part of the inner ring area to a depth of 2.4 m with 20 cm depth sections. The soil samples were packed in polythene bags and were processed and analysed in the laboratory for moisture and tritium content in soil. The moisture content of the soil sample was estimated by gravimetric technique. Soil moisture was recovered using vacuum distillation process and tritium concentration of soil moisture

was determined using liquid scintillation counter for soil cores of various depths.

Results

Point potential measurements

The changes in potential field at every grid nodal point were measured before and during the infiltration test. It was expected that the water flux front at and below the soil surface would effect changes in the potential field

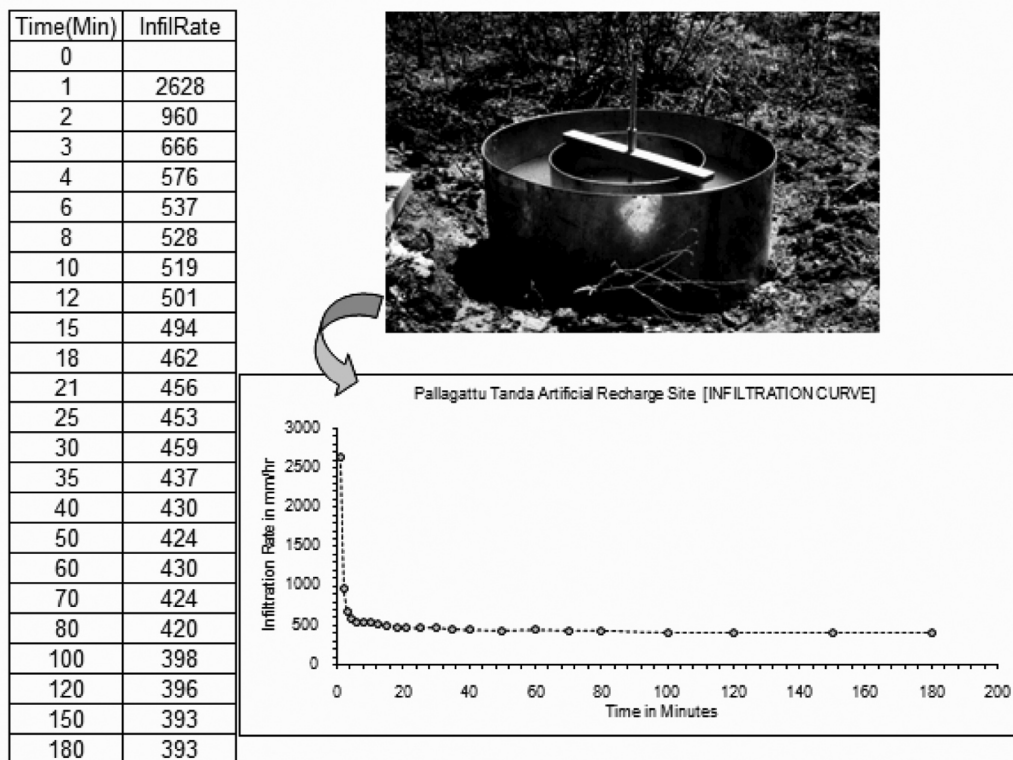


Figure 2. Infiltration test set-up and resultant curve. Duration of test: 180 min. Tracer used for simulation test: (1) 20 ml of 30 microcurie/ml tritium (inner ring).

and the change varies with time as the percolation advances. As mentioned earlier, one of the non-polarized electrodes placed at infinity remained undisturbed throughout the duration of the experiment. The other electrode was moved over the nodal points at different profile lines as shown (Figure 1). The potential measurement during the infiltration test was repeated in all grid nodal points at 15, 30, 45, 60, 90, 120 and 180 min interval covering the entire duration of the experiment.

A potential gradient measurement was attempted at the E-profile by keeping one of the electrodes fixed at the starting, and moving the other electrode away along the profile. The mid-point was taken as the observed point of location, i.e. 0.25, 0.75, 1.25 and so on, for the entire grid line of the E-profile. Measurements were extended beyond the grid to facilitate to achieve observation up to 3.75. The measured potential values were directly used for analysis. As the experiment progressed, a reduction in potential was observed till the 45th minute, at the location of infiltrometer placement, to a radial distance of 1 m from the centre, indicating probably the advancement of water flux in a conical shape. Similarly, to observe the variations in SP due to infiltration another attempt was made by correcting the SP data of different time intervals to the initial set of data (0th minute). The corrected data to the initial state (0th minute) of the E-profile was plotted for different time intervals as shown in Figure 3 a.

Figure 3 a also indicates that the SP variation is significant from the 45th minute onwards. However, there is a significant increase in negative potential at the centre and a gradual increase towards positive polarity on either sides, beyond 2 m of the profile line. This probably indicates that the movement of moisture flux is deeper at the centre than towards the lateral extent. Revil *et al.*²² discussed the self-potential signals associated with pumping of a well dataset of Bogoslovski and Ogilvy²³ – the presence of a drainage ditch near the pumping well caused a relatively distinct negative polarity and positive polarity due to lowering of water level at the pumping well site. In another study, the negative anomalies observed on the flanks of volcanoes were said to be associated with rainfall percolation²⁴. The observed changes in the potential field during the present experiment may be attributed to the dominant movement of moisture vertically downwards. However, beyond the 45th minute observation, the potential field started increasing at the central nodal points and in the adjoining areas, indicating a change in flow movement/direction. Similar features were observed in profiles D and C at the north of the E-profile at distances of 0.5 and 1 m. However, in profiles F and G towards the south of the E-profile, this feature was found to be insignificant.

In order to understand the changes in potential field with time due to moving moisture flux during the

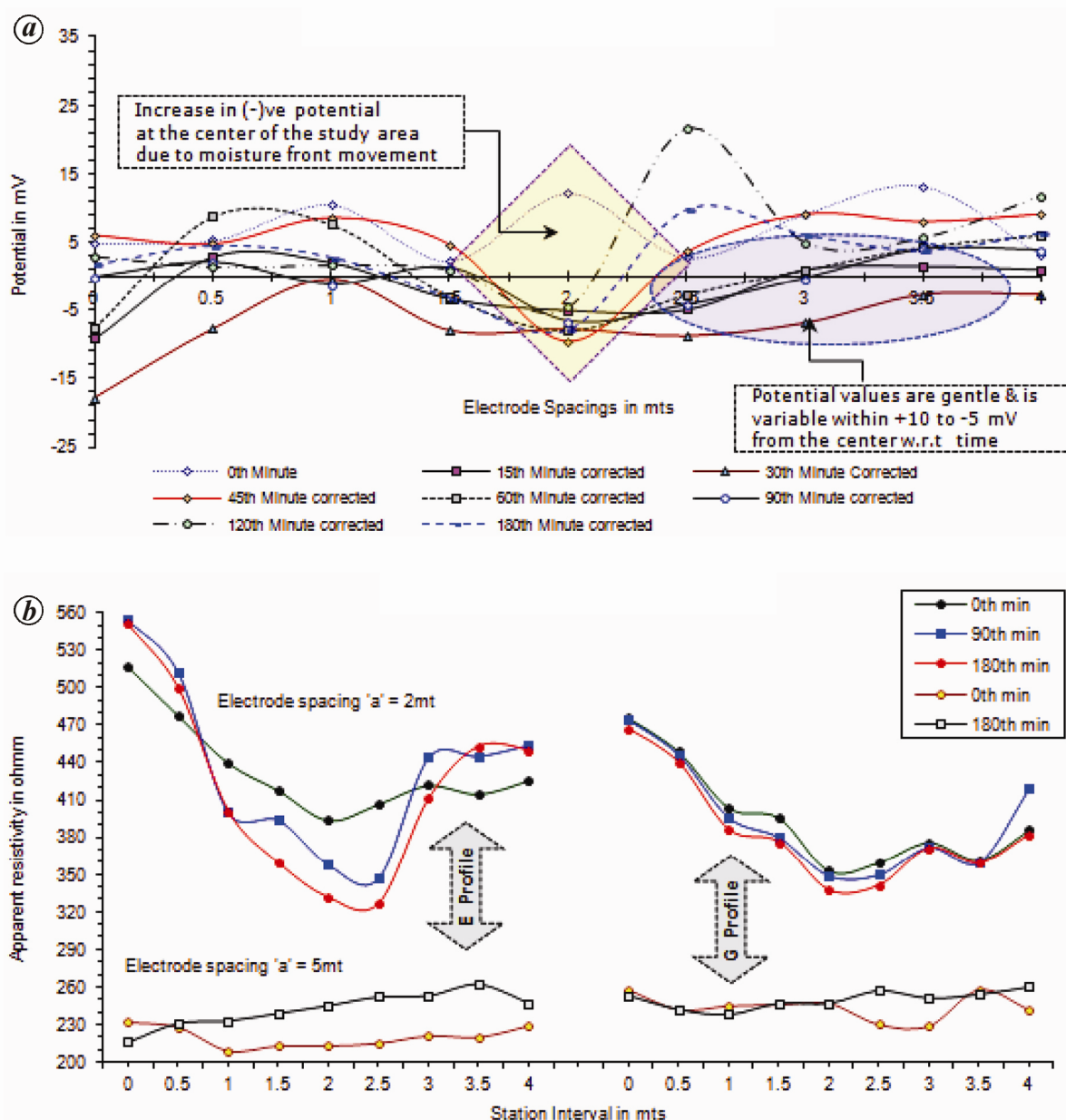


Figure 3. a, Corrected apparent potential measurement along E-profile. b, Apparent resistivity difference between zero and 180 minute observations along profiles E and G.

infiltration test over the entire study grid area, an attempt was made to draw contours considering all the measured potential values of all nodal points at a given time. The potential contours thus prepared for the time intervals 0, 15, 30, 45, 60, 90, 120 and 180 min are shown in Figure 4. The contour behaviour indicates that the moisture flux probably moves in a northwesterly direction from the 45th minute onwards till the end of the experiment. There was a gradual reduction in potential as the infiltration process progressed in this direction. Similarly, the contours of difference in potential calculated between two successive measurement time intervals for all nodal

points were studied to further understand the behaviour of moisture flux. This way the analysis also concurred with the earlier inference of moisture flux moving in a northwesterly direction after the 45th minute of the infiltration experiment.

Resistivity measurements

Changes in electrical properties are expected when the soil saturates. To measure such changes in terms of resistivity of the sub-surface formation at the infiltration area, electrical method is the best suited geophysical tool.

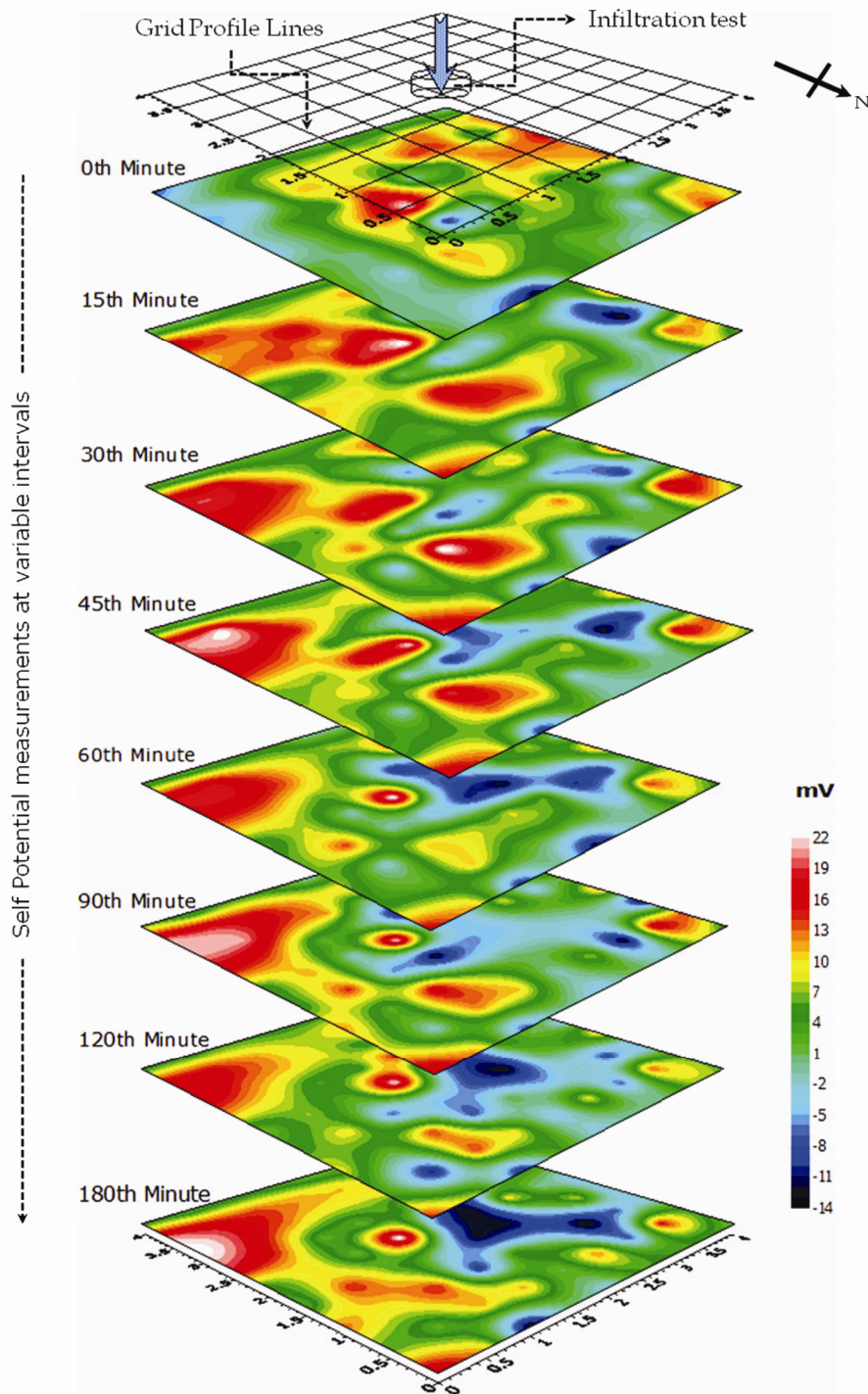


Figure 4. Planar view on observed self-potential variations at different time periods.

Among electrical methods, the vertical electrical sounding and lateral profiling techniques are commonly deployed. Vertical electrical sounding is adopted to investigate changes in the earth resistivity with depth at a particular point. However, profiling is preferred to map lateral variations in resistivity within a limited depth range along a line. Earlier studies on monitoring ground-

water flow by mapping the electrical response to an injected saline tracer, either solely from the ground surface²⁵⁻²⁸ or in boreholes²⁹ indicated that the changes in electrical properties of the sub-surface due to the movement of a natural or injected fluid can be a better tool for understanding the pathways. Electrical resistivity tomography results have been elucidated for characterizing

sub-surface solute transport in a heterogeneous sand and gravel aquifer³⁰. As the percolating moisture front influences the resistivity of sub-surface, Wenner profiling with electrode spacing of $a = 2$ m and $a = 5$ m was adopted along the profile lines of A, C, E, G and H as shown in Figure 1. These two spacings were selected as the expected downward movement of water would not be more than 3 m within the planned infiltration experiment of 3 hours. The profiling was conducted at time intervals of 0, 90 and 180 min of the experiment at alternate profile lines and was conducted such that the measurements did not interfere with natural SP measurements. The variations observed in these three time-domains are plotted and shown for the E-profile in Figure 3 *b*.

Analysis carried out to understand the resistivity change in the sub-surface formation due to infiltrating water was found to be significant. The difference in apparent resistivity between the starting (0th minute) and closing time (180th minute) of the infiltration test was calculated for the two spacing intervals of $a = 2$ m and $a = 5$ m separately. The observation for the 2 m electrode spacing showed reduction in apparent resistivity to the order of 80 Ω -m at the central part below the infiltrometer placement (E-profile). Whereas apparent resistivity of the same profile for 5 m electrode separation, showed an increase to the order of 20–40 Ω -m. Similarly, lowering of apparent resistivity to a lesser extent for the 2 m electrode separation and increase in apparent resistivity for the 5 m electrode separation were observed in profile G on the southern side of the E-profile line as shown in Figure 3 *b*. However, on the northern side, along the profile line C, the resistivity continued to decrease depicting the influence of moving moisture front. The observed significant reduction between nodal points 3 and 4 indicates the influence of moisture on the northwestern part. This observation concurs with the SP indication of percolating waterfront, initially dominated by vertical flow and later on through preferred flow path towards the north-western side at deeper levels.

Tritium tracer confirmative studies

Having deciphered the direction of water flux after a certain lapse of time from the SP transient survey and resistivity profiling, it was felt necessary to confirm the findings by studying the tritium tracer distribution along the direction of movement. In order to study the distribution of tracer in soils, and to understand the vertical downward movement, vertical soil core at the centre (E-2) of the infiltration ring was collected up to a depth of 240 cm at 20 cm intervals using auger, at the end of the infiltration test. These soil samples were subjected to laboratory analysis for the determination of moisture content and tritium concentration in soil moisture. The vertical variation in tritium concentration was plotted against

the depth. The tritium peak (center of gravity) was found to be at a depth of 188.5 cm indicating a displacement/movement of tracer from the ground level. The movement of the tracer took place over the infiltration test period of 180 min resulting in ~ 1 cm downward movement per minute. Soil cores at nodal points C-2, C-6, E-0 and H-0 were also collected for studying the lateral movement of the tracer. However, due to the collapsible nature of soil encountered during the coring, the collection was possible only up to 170 cm depth at H-0 nodal point and up to 90 cm in the rest of the nodal points. The tritium concentration in all these profiles is significantly lower (< 100 CPM) indicating a limited spread of moving moisture front.

In order to confirm the northwesterly movement of water flux depth, an 'L' shaped trench of width 1.0 m and depth 3.6 m was excavated between A and C profiles for the entire 4 m on the northern side. Another L shaped trench was excavated in the north–south direction covering the grid area from A 3–4 to I 3–4, after 24 h of the infiltration experiment. Soil core samples on the wall side of the C profile line were scooped out at every 20 cm interval from the top at C-1.5, 2.5 and 3 nodal positions to an excavated depth of 360 cm. The positions of soil profiles collected are shown in Figure 1. Similarly, soil samples at 20 cm interval were also collected on a horizontal section at a depth of 2.5 m on the wall side of the C profile line at the contact point of the soil and weathered granite along the east–west section. The position of this horizontal collection line is also shown in Figure 1. The soil moisture was analysed for tritium content. The tritium tracer distribution with depth at all profiles is shown in Figure 5. It is very clear from the tritium profiles that the profile at C-3 has high content of tritium in soil moisture from a depth of 140 cm and attains maximum concentration of 14000 CPM at a depth of 220–240 cm which is 42 cm deeper than the centre profile of 188 cm. However, in the other vertical profiles C-1.5 and 2.5, the tritium content in soil moisture is below 100 CPM, indicating least influence of moisture flux in this direction as seen in Figure 5. The soil moisture tritium content of the horizontal profile showed a very high content of tritium on the western end of the profile concurring with the result of profile C-3.

Discussion

The infiltration rate at different time intervals given in a tabular form (Figure 2) clearly indicates that from the 40th minute onwards, the process of infiltration attained a more or less steady state of ~ 430 mm/h. However, the observed data indicates that the rate further reduced after the 80th minute to a level of 390 mm/h indicating probable changes in the deep percolation process. The PP at every 15 min interval clearly depicts a change in the

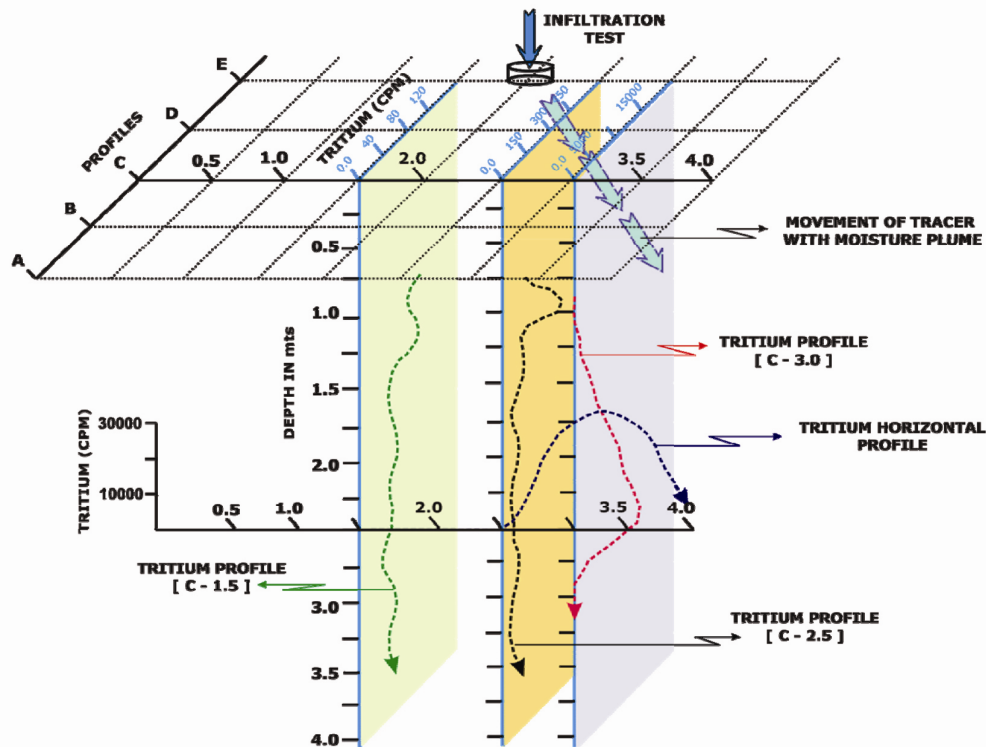


Figure 5. Tritium tracer distribution with depth at selected profiles.

potential field strength and direction of movement after the 45th minute. This reflects the observation made in the infiltration rate. The electrodes were neutralized by placing them in a saturated ditch for a considerably long duration (360 min) before starting the survey. This was further strengthened by the point potential contour behaviour at the 90th and 180th min, indicating qualitatively the influence of moving moisture flux towards the northwest corner, which explains the observed change in infiltration rate after the 80th minute.

Having known the direction of transient moisture flux movement qualitatively, the tracer studies further confirmed the depth and direction. The tracer migration at E-2, i.e. the centre of the infiltrometer was estimated to be 188.5 cm which allowed us to calculate the average permeability of the test site. Using the displacement of the tracer and experiment time of 180 min, the vertical permeability of the soil was calculated as 1.05 cm/min. Similarly, from the analysis of tritium distribution in C-3 of the trench profile, the displacement of the tracer from surface at E-2 (centre) to C-3 (to a depth of 230 cm) and considering the hypotenuse, the distance travelled by the tracer was calculated as 270 cm. Taking the distance of 270 cm and time of 180 min, the estimated permeability in that direction is about 1.5 cm/min.

The resistivity profiling at the beginning and the end of the infiltration test brought out a clear picture on changes induced due to infiltrating water. The two separations followed are intended to map the changes down to a depth

of 3 m. The theoretical estimation of the effective depth of investigation for Wenner configuration is about 0.29 times of the current electrode distance from the centre of the array³¹. In the present study the electrode spacing of $a = 2$ m and $a = 5$ m was found to be adequate to map the apparent resistivity changes along the profile lines. Based on the transient changes in apparent resistivity due to infiltration process, the influence due to moisture spread was seen as half-lensoidal with more influence at the centre (reduction in resistivity of 30–80 Ω -m) and less influence at the border (reduction in resistivity of 10–20 Ω -m) of the study grid area. As the time of the infiltration process increased, the change in direction of percolation towards the NW corner of the study area is clearly mapped under the 5 m electrode separation due to the reduction in resistivity (40 Ω -m) at profile line C 3–4. This finding later concurred with the SP mapping. Using the effective depth of 0.29 times of current electrode separation for $a = 5$ m profile, the information obtained for the profile line C worked out to be 2.175 m. The tracer profile of C-3 also indicated that the tracer moved to a depth of 220–240 cm concurring with the resistivity findings of depth and direction.

Conclusions

The study of tracing moisture flux in the unsaturated zone using SP method clearly indicates that the subsurface movement of moisture flux is not necessarily vertically

downwards till it reaches the saturated zone. The direction of moving flux can be traced through transient SP measurements and the preferential direction delineated, can be confirmed through transient resistivity profiling and tracer studies. The experiment mainly demonstrates that the SP studies would be useful in understanding the natural recharge process of regional variability and in mapping the pathways of contaminants from industrial waste dump sites and land fills moving along with percolating water. It is plausible to determine the average permeability of the soil by combining the infiltration and tracer applications without disturbing the soil conditions.

1. Ahmad, U., A laboratory study of streaming potentials. *Geophys. Prospect.*, 1964, **XII**, 49–62.
2. Mitzutani, H., Ishido, T., Yokokura, T. and Ohnishi, S., Electrokinetic phenomena associated with earthquakes. *Geophys. Res. Lett.*, 1976, **3**, 365–368.
3. Ishido, T., Self-potential generation by subsurface water flows through electrokinetic coupling, detection of subsurface flow phenomena. In *Lecture Notes in Earth Science*, 27, Springer, New York, 1989, pp. 121–131.
4. Morat, P. and Le Mouél, J. L., Signaux électriques engendrés par des variations de contrainte dans des roches poreuses non saturées. *C. R. Acad. Sci. Paris, Ser. II*, 1992, **315**, 955–963.
5. Aubert, M. and Dana, I., Interpretation of the self-potential radial profiles in vulcanology. Possibilities of the SP method for monitoring the active volcanoes. *Bull. Soc. Geol. France*, 1994, **165**, 113–122.
6. Hashimoto, T. and Tanaka, Y., A large self-potential anomaly on Unzen volcano, Shimabara peninsula, Kyushu island, Japan. *Geophys. Res. Lett.*, 1995, **22**, 191–194.
7. Perrier, F., Trique, M., Lorne, B., Avouac, J. P., Hautot, S. and Tarits, P., Electrical variations associated with yearly lake level variations. *Geophys. Res. Lett.*, 1998, **25**, 1955–1958.
8. Kelly, W. E., Geoelectric sounding for estimating hydraulic conductivity. *Ground Water*, 1977, **15**(6), 420–425.
9. Kosinski, W. K. and Kelly, W. E., Geoelectric soundings for predicting aquifer properties. *Ground Water*, 1981, **19**(2), 163–171.
10. Niwas, S. and Singal, D. C., Aquifer transmissivity of porous media from resistivity data. *J. Hydrol.*, 1985, **82**, 143–153.
11. Ponzoni, G., Ostroman, A. and Molinari, M., Empirical relation between electrical transverse resistance and hydraulic transmissivity. *Geoexploration*, 1984, **22**, 1–15.
12. Revil, A., Hermitte, D., Voltz, M., Moussa, R., Lacas, J.-G., Bourrie, G. and Trolard, F., Self-potential signals associated with variations of the hydraulic head during an infiltration experiment. *Geophys. Res. Lett.*, 2002, **29**(7), 10-1–10-4.
13. SAILHAC, P., DARNET, M. and MARQUIS, G., Electrical streaming potential measured at the ground surface: forward modeling and inversion issues for monitoring infiltration and characterizing the Vadose zone. *Vadose Zone J.*, 2004, **3**, 1200–1206.
14. Doussan, C., Jouniaux, L. and Thony, J.-L., Variations of self-potential and unsaturated water flow with time in sandy loam and clay loam soils. *J. Hydrol.*, 2002, **267**, 173–185.
15. Perrier, F., Trique, M., Aupiais, J., Gautam, U. and Shrestha, P., Electric potential variations associated with periodic spring discharge in western Nepal. *CR Acad. Sci. Paris, Ser. II3*, 1999, **28**, 73–79.
16. Jouniaux, L., Bernard, M. L., Zamora, M. and Pozzi, J. P., Streaming potential in volcanic rocks from Mount Pelée. *J. Geophys. Res.*, 2000, **105**(B4), 8391–8401.
17. Jouniaux, L. and Pozzi, J.-P., Permeability dependence of streaming potential in rocks for various fluid conductivities. *Geophys. Res. Lett.*, 1995, **22**, 485–488.
18. Thony, J. L., Morat, P., Vachaud, G. and Le Mouél, J.-L., Field characterization of the relationship between electrical potential gradient and soil water flux. *Earth Planet. Sci.*, 1997, **325**, 317–321.
19. Richards, L. A., Capillary conduction of liquids through porous medium. *Physics*, 1931, **1**, 318–313.
20. Horton, R. E., An approach towards physical interpretation of infiltration-capacity. *Soil Sci. Soc. Am. Proc.*, 1940, **5**, 399–417.
21. Rangarajan, R. and Athavale, R. N., Annual replenishable ground water potential of India—an estimate based on injected tritium studies. *J. Hydrol.*, 2000, **234**, 38–53.
22. Revil, A., Naudet, V., Nouzaret, J. and Pessel, M., Principles of electrography applied to self-potential electrokinetic sources and hydrogeological applications. *Water Resour. Res.*, 2003, **39**(5), 1114.
23. Bogoslovsky, V. A. and Ogilvy, A. A., Natural potential anomalies as a quantitative index of the rate of seepage from water reservoirs. *Geophys. Prospect.*, 1970, **18**, 261–268.
24. Xavier, G., Jouniaux, L. and Pozzi, J.-P., Streaming potentials of sand column in partial saturation conditions. *J. Geophys. Res.*, 2003, **108**(B3), 2141; doi:10.1029/2001JB001517.
25. White, P. A., Measurement of ground-water parameters using salt-water injection and surface resistivity. *Groundwater*, 1988, **26**, 179–186.
26. White, P. A., Electrode arrays for measuring groundwater flow direction and velocity. *Geophysics*, 1994, **59**, 192–201.
27. Osiensky, J. L. and Donaldson, P. R., Electrical flow through an aquifer for contaminant source leak detection and delineation of plume evolution. *J. Hydrol.*, 1995, **169**, 243–263.
28. Morris, M., Rønning, J. S. and Lile, O. B., Geoelectric monitoring of a tracer injection experiment: modeling and interpretation. *Eur. J. Environ. Eng. Geophys.*, 1996, **1**, 15–34.
29. Bevc, D. and Morrison, H. F., Borehole-to-surface electrical resistivity monitoring of salt water injection experiment. *Geophysics*, 1991, **56**, 769–777.
30. Kemna, A., Vanderborght, J., Kulesa, B. and Vereecken, H., Imaging and characterization of subsurface solute transport using electrical resistivity tomography (ERT) and equivalent transport models. *J. Hydrol.*, 2002, **267**, 125–146.
31. Appa Rao, A., *Developments in Geoelectrical Methods*, Oxford Publishing Co Pvt Ltd, 1997, pp. 1–314.

ACKNOWLEDGEMENTS. We thank the Director, National Geophysical Research Institute for support in carrying out the research activity. The support of Government of India through Planning Commission under task force activity on ‘Development of techniques and methodologies for exploration, assessment and management of groundwater in hard rock areas’ is acknowledged. We also thank Director, CWPRS for his encouragement in publishing this manuscript.

Received 1 June 2017; revised accepted 4 December 2017

doi: 10.18520/cs/v114/i07/1414-1422